

## Research Article

# Nonlinear Displacement of the Electrothermal V-Shaped Actuator

Truong Duc Phuc,<sup>1</sup> Phuc Hong Pham ,<sup>1</sup> Kien Trung Hoang ,<sup>2</sup> and Bui Ngoc-Tam <sup>3</sup>

<sup>1</sup>Hanoi University of Science and Technology, Hanoi, Vietnam

<sup>2</sup>Le Quy Don Technical University, Hanoi, Vietnam

<sup>3</sup>Shibaura Institute of Technology, Tokyo, Japan

Correspondence should be addressed to Phuc Hong Pham; [phuc.phamhong@hust.edu.vn](mailto:phuc.phamhong@hust.edu.vn) and Kien Trung Hoang; [kienhoangtrung87@gmail.com](mailto:kienhoangtrung87@gmail.com)

Received 8 December 2023; Revised 28 February 2024; Accepted 17 April 2024; Published 2 May 2024

Academic Editor: Jinxin Liu

Copyright © 2024 Truong Duc Phuc et al. This is an open access article distributed under the Creative Commons Attribution License, which permits unrestricted use, distribution, and reproduction in any medium, provided the original work is properly cited.

This article proposes a formula for calculating the nonlinear displacement of the electrothermal V-shaped actuator aims to determine more accurately its displacement. The nonlinear displacement model is established based on the axial deformation of V-beams with two fixed ends. Hence, the theoretical displacements of a particular V-shaped actuator (i.e. dimension as beam length of  $750\ \mu\text{m}$ ; beam width of  $6\ \mu\text{m}$ ; beam thickness of  $30\ \mu\text{m}$ ; inclined angle of  $2^\circ$ ) are compared with the simulation and experimental results. The evaluation shows that our calculation error compared with the simulation and experiment is less than 5% and 12.4%, respectively. This confirmed the advantages of the proposed formula according to the nonlinear displacement model. This work provides a theoretical model for predicting more precisely the displacement of a V-shaped actuator. The advantage of this model is that it will significantly reduce the time in the design and trial manufacturing process.

## 1. Introduction

Electrothermal actuator (ETA) is a type of MEMS (micro electro-mechanical systems) device that works on the principle of converting electrical energy into heat and thermal expansion. Among them, the V-shaped beam is the most widely being used, due to the outstanding advantages such as large driving force, small driving voltage, simple structure, larger displacement-to-size ratio compared to others as mentioned in [1, 2]. Currently, the electrothermal V-shaped actuators (EVA) are frequently used in driving micromechanical systems such as microgrippers [3], micromotors [4], nanomaterial testing devices [5] or thermal safe devices [6], etc.

Accurately calculating displacement of the V-shaped actuator according to the change of driving voltage is always an important problem because it supports selecting the dimensions of the microdevices relating design and trial fabrication processes. Therefore, finding a method or

formula to calculate accurately the nonlinear displacement of the V-shaped actuator under the influence of both thermal and mechanical deformation is quite needed.

Research on using mathematical methods to describe the heat transfer process of EVA has been developed recently. Direct analytical methods have been used to model steady state heat transfer [7], or transient heat transfer [8]. The finite difference heat transfer model was used to determine the change and distribution of temperature on the V-beam as shown in [9, 10]. These works have provided methods for calculating more precisely the temperature distribution on the thin beam. However, the nonlinear deformation of the V-beam has not been considered when determining the displacement of the EVA. In publications [11, 12], we have applied the finite difference model to calculate more exactly the thermal expansion force of the EVA, but the displacement is examined by the linear formula, so the tolerance is still quite large.

In practice, the displacement of EVA often needs to be large and leads to a nonlinear stress-displacement relationship of the V-beams. The development of a nonlinear displacement model of the V-beam allows to determine more accurately the displacement of the actuator. This is essential as well as valuable to predict accurately the displacement of microdevices, likes in measuring mechanical properties of micron specimens [13] or in electrical switches [14]. In [15], the authors have proposed a thermal strain model by direct analysis method, in which has considered the first-order nonlinear strain-displacement relationship. The results of this model are used to predict the maximum stress on the beam to avoid plastic deformation. However, the nonlinear model can only determine the displacement according to the average temperature on the beam and is applicable to the V-beam made of nickel material.

This work establishes a nonlinear displacement model of the EVA by analytical method. Additionally, this nonlinear model is also combined with the nonlinear heat transfer model developed by the finite difference method as mentioned in [11, 12]. The integration of two models will allow determining more accurately the displacement of the EVA when considering the nonlinear mechanical deformation of the parallel V-beam system fabricated from silicon by traditional SOI-MEMS technology. The result helps the designers easily select the applied voltages as well as accurate dimensions of the driving V-shaped actuator, aims to obtain an appropriate displacement for the working requirements of MEMS devices such as microgripper, micromotor or microconveyor systems.

## 2. Linear and Nonlinear Models of the EVA

**2.1. Structure and Linear Displacement Formula.** The structure of a typical EVA is shown in Figure 1. This actuator consists of the central shuttle (1) suspended by pairs of V-shaped inclined beams (2); the other ends of these beams are attached to two fixed electrodes (3). The dimensions and geometrical parameters are denoted as follows:  $L$ ,  $w$  and  $h$  are the length, width and thickness of the beam, respectively;  $\theta$  is the inclined angle of the beam relative to  $X$  direction;  $g_a$  is the gap between the structural layer and the substrate (i.e. the  $\text{SiO}_2$  buffer layer of the Silicon on Insulator-SOI wafer);  $n$  is the number of V-beam pairs.

When a voltage is applied on two fixed electrodes, the current will transmit through the beams and generate heat as well as induce the expansion of V-beam, a total expansion force pushes the central shuttle to move in  $Y$  direction. If the voltage is down to zero, the temperature on the beams gradually decreases; the beams will shrink and pull the shuttle back to its original position.

Let  $K$  be the equivalent stiffness of the V-beam system, it is determined as follows [12]:

$$K = \frac{2nE(12I \cos^2 \theta + AL^2 \sin^2 \theta)}{L^3}, \quad (1)$$

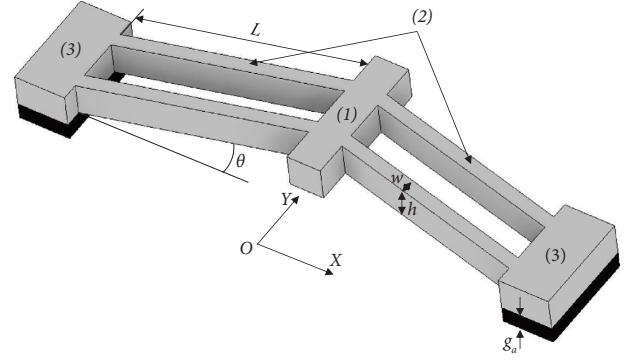


FIGURE 1: Schematic of the EVA. (1) The central shuttle; (2) V-shaped beams; (3) fixed electrodes.

where  $I = hw^3/12$  is the inertia moment of beam cross-sectional area,  $A = h \cdot w$  is the area of beam cross-section,  $E = 169$  GPa is a Young's modulus of silicon.

The static displacement of the EVA is determined by

$$Y_0 = \frac{F}{K}. \quad (2)$$

Here,  $F$  is the total heat expansion force acting on the shuttle in  $Y$  direction [12]:

$$F = 2nAE \frac{\Delta L}{L} \sin \theta. \quad (3)$$

$\Delta L$  is the thermal expansion of a beam.

By substituting (3) and (1) into (2), we have a linear displacement as follows:

$$Y_0 = \frac{AL^2}{12I \cos^2 \theta + AL^2 \sin^2 \theta} \Delta L \sin \theta. \quad (4)$$

It is clear that the linear displacement  $Y_0$  depends on the thermal expansion length  $\Delta L$  as well as the geometry parameters of beam like the length  $L$ , the width  $w$  and the inclined angle  $\theta$ .

**2.2. Calculation of Nonlinear Displacement.** In case the V-beam fixed at both ends, when the displacement is large enough, the length of the deformation curve is longer than the original length of the beam. Hence, there is an additional axial force against the long deformation and causes a greater stiffness of the beam. In other words, the practical displacement of the beam will be smaller than the value calculated by the linear formula (4).

Considering the fixed-end V-beam is loaded by a concentrated force with magnitude  $2P$  at the center of the shuttle as shown in Figure 2.

Due to symmetrical structure, we need only to consider the forces acting on the left half of the V-beam (Figure 3):

The assumptions used to establish the nonlinear displacement model including: the beam works in the linear elastic domain of material; the deformation of beam elements is small ( $dy/dx \ll 1$ ).

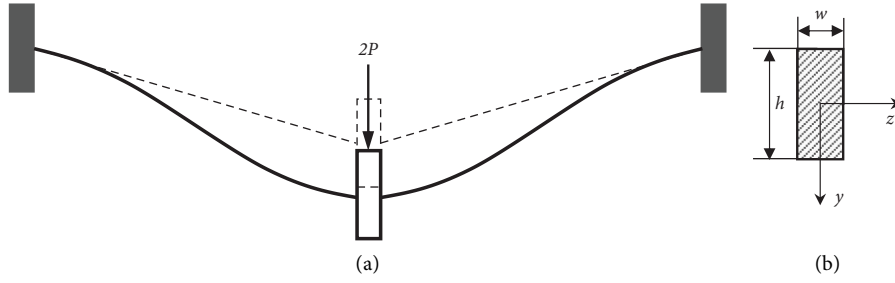


FIGURE 2: Nonlinear deformation of the V-beam. (a) Deformation of V-beam; (b) cross-section area of the beam.

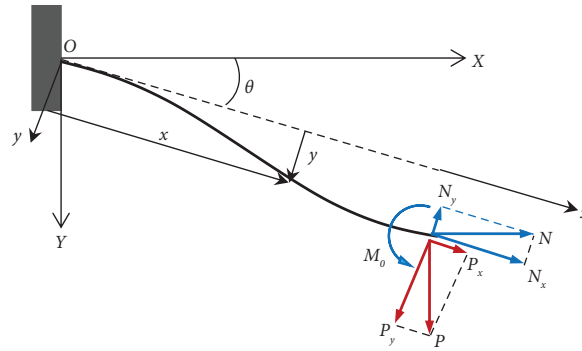


FIGURE 3: Scheme of load and reaction forces acting on a half of the V-beam.

From Bernoulli-Euler law and neglecting the square of the slope  $(dx/dy)^2$ , the displacement differential equation of the beam in  $y$ -direction according to local coordinate  $Oxy$  (see Figure 3) is established:

$$EI \frac{d^2 y}{dx^2} = (P \cos \theta - N \sin \theta) \cdot (L - x) - (N \cos \theta + P \sin \theta) \cdot y - M_0, \quad (5)$$

where  $M_0$  is a reaction moment between the half-beam and the shuttle,  $N$  is an axial reaction force due to beam stretched.

The general solution of the differential (5) will be

$$y(x) = C_1 \cosh \lambda x + C_2 \sinh \lambda x + A_1 x + B_1. \quad (6)$$

From (5) and (6), we have

$$A_1 = -\frac{P \cos \theta - N \sin \theta}{N \cos \theta + P \sin \theta}; \quad B_1 = -\frac{M_0 - (P \cos \theta - N \sin \theta)L}{N \cos \theta + P \sin \theta}; \quad \lambda = \sqrt{\frac{N \cos \theta + P \sin \theta}{EI}} \quad (7)$$

Here,  $C_1$  and  $C_2$  are the constants determined from boundary conditions:  $(dy/dx)|_{x=0} = 0$ ;  $(dy/dx)|_{x=L} = 0$ ; and can be expressed as follows:

$$C_1 = \left( \frac{P \cos \theta - N \sin \theta}{N \cos \theta + P \sin \theta} \right) \cdot \left( \frac{1 - \cosh \lambda L}{\lambda \sinh \lambda L} \right) = \frac{P \cos \theta - N \sin \theta}{\lambda (N \cos \theta + P \sin \theta)} \cdot \tanh \left( \frac{\lambda L}{2} \right), \quad (8)$$

$$C_2 = -\frac{A_1}{\lambda} = \frac{P \cos \theta - N \sin \theta}{\lambda (N \cos \theta + P \sin \theta)}. \quad (9)$$

To find the value of  $M_0$ , we use the boundary condition:  
 $y|_{x=0} = 0$ .

$$M_0 = \frac{(P \cos \theta - N \sin \theta)}{\lambda} \cdot \left( \lambda L - \tanh \left( \frac{\lambda L}{2} \right) \right). \quad (10)$$

The function of  $y$ -displacement can be determined by substituting  $A_1$ ,  $B_1$ ,  $C_1$ ,  $C_2$  and  $M_0$  into (6):

$$y(x) = \frac{P \cos \theta - N \sin \theta}{\lambda (N \cos \theta + P \sin \theta)} \cdot \left[ \sinh \lambda x - \tanh \left( \frac{\lambda L}{2} \right) \cdot (\cosh \lambda x - 1) - \lambda x \right]. \quad (11)$$

When the deformation of the beam element is small enough (i.e. the ratio  $(dy/dx) \ll 1$ ), the axial expansion of the beam can be approximated as follows:

$$\Delta L = L' - L = \int_0^L \left[ 1 + \left( \frac{dy}{dx} \right)^2 \right]^{(1/2)} dx - L, \quad (12)$$

$$\text{Or: } \Delta L \approx \int_0^L \left[ 1 + \frac{1}{2} \left( \frac{dy}{dx} \right)^2 \right] - L = \frac{1}{2} \int_0^L \left( \frac{dy}{dx} \right)^2 dx, \quad (13)$$

According to scheme in Figure 3, the axial reaction force is determined as follows:

$$N = \frac{1}{\cos \theta} \cdot \left( A.E. \frac{\Delta L}{L} - P \sin \theta \right). \quad (14)$$

From (7)–(9), we have

$$(N \cos \theta + P \sin \theta)^3 = \frac{A.E. (P \cos \theta - N \sin \theta)^2}{2} \cdot \left( \frac{3}{2} - \frac{1}{2} \tanh^2 u - \frac{3}{2} \frac{\tanh u}{u} \right), \quad (15)$$

where  $u = \lambda L/2$

From  $(N \cos \theta + P \sin \theta = EI\lambda^2)$  and (10), we have

$$P \cos \theta - N \sin \theta = \frac{8E.I. (2I/A)^{(1/2)}}{L^3} \cdot u^3 \cdot \left( \frac{3}{2} - \frac{1}{2} \tanh^2 u - \frac{3}{2} \frac{\tanh u}{u} \right)^{(1/2)}. \quad (16)$$

With  $[N \sin \theta = (4E.I.u^2/L^2 - P \sin \theta) \cdot \tan \theta]$  and the (16), we infer:

$$P = \frac{4E.I.u^2}{L^2} \cdot \sin \theta + \frac{8E.I. (2I/A)^{(1/2)} \cdot u^3 \cdot \cos \theta}{L^3} \cdot \left( \frac{3}{2} - \frac{1}{2} \tanh^2 u - \frac{3}{2} \frac{\tanh u}{u} \right)^{(1/2)}. \quad (17)$$

By substituting (10) and (11) into (7), the maximum  $y$ -displacement at the center of V-beam is determined as follows:

$$y_{\max} = 2 \left( \frac{2I}{A} \right)^{(1/2)} \cdot (u - \tanh u) \cdot \left( \frac{3}{2} - \frac{1}{2} \tanh^2 u - \frac{3}{2} \frac{\tanh u}{u} \right)^{-(1/2)}. \quad (18)$$

From (17) the variable  $u$  will be solved and then substituting  $u$  into (13), we will obtain the value of  $y_{\max}$ .

Finally, the displacement of the shuttle in  $Y$  direction (i.e. in vertical direction) can be calculated as follows:

$$Y_1 = \frac{y_{\max}}{\cos \theta} = \frac{2}{\cos \theta} \left( \frac{2I}{A} \right)^{(1/2)} \cdot (u - \tanh u) \cdot \left( \frac{3}{2} - \frac{1}{2} \tanh^2 u - \frac{3}{2} \frac{\tanh u}{u} \right)^{-(1/2)}. \quad (19)$$

It shows that the nonlinear displacement  $Y_1$  also depends on the geometry dimensions of the beam as  $L$ ,  $w$ ,  $h$ , and  $\theta$ . Besides, it is influenced by eigenvalue  $u$  or  $\lambda$  determined from transcendental (17).

### 3. Fabrication and Measurement

**3.1. Fabrication Process.** The V-shaped microactuator has been fabricated using SOI-MEMS technology and a silicon-on-insulator wafer with 3 layers including structural silicon layer, SiO<sub>2</sub> buffer and substrate with thicknesses of 30  $\mu\text{m}$ , 4  $\mu\text{m}$  and 450  $\mu\text{m}$ , respectively. The fabrication process includes 5 main steps as shown in Figure 4: cleaning the SOI wafer (Figure 4(a)); photolithography and developing (Figure 4(b)); deep reactive ion etching (Figure 4(c)); cutting and removing photoresist (Figure 4(d)); vapor HF etching (Figure 4(e)). Figure 5 is a SEM (scanning electron microscope) image of one EVA structure with 10 parallel V-beam pairs after fabrication.

**3.2. Measurement.** The diagram of the displacement measuring system is illustrated as in Figure 6. The system consists of a functional generator, amplifier, optical microscope and CCD camera (all are mounted on an anti-vibration table). The microactuator is located on the stage of the microscope, camera is used to record the operation of EVA at various applied voltages.

Each displacement value of the shuttle is determined relatively through the number of pixels on an image corresponding to a certain voltage value. The number of measured pixels will be proportional to the number of pixels of the specific dimension of EVA (example: predesigned dimension such as the width of shuttle - 100  $\mu\text{m}$  corresponding to about 400 pixels on the picture, please see more in Figure 7). From which the experimental displacement can be inferred.

### 4. Result and Discussion

The EVA structures have been successfully fabricated from SOI wafer. The geometry dimensions of this EVA are given in Table 1.

The material parameters of the silicon device layer are listed in Tables 2 and 3.

The 3D finite element model of the V-shaped beam (with the dimensions, material properties and ambient given in Tables 1–3) was established by ANSYS WORKBENCH 15. The model is meshed with a body size of 10 micrometers in both thermal-electric and static-structural to simulate the nonlinear displacement of the V-shaped beam in the settings of the Static-Structural model and selecting the large deformation function. This is a development/difference from the linear simulation of the previous publications.

The calculation results and comparison of displacements in both of linear and nonlinear are shown in Figure 8. The simulation results of nonlinear displacement with thermal expansion force acting on the beam at the voltage of 16 V as shown in Figure 9. Finally, the comparison of nonlinear displacements calculated by the formula (19) and ANSYS-simulated are shown in Figure 10.

As the displacement results are shown in Figure 8, it is easy to see that there is a significant deviation between linear and nonlinear formulas while applied voltage is larger than 6 V. The calculated nonlinear displacement (using formula number 14) increases gradually with the driving voltage and is much smaller when compared with the linear displacement (formula number 4) at the same applying voltage. As an example, at the voltage of 12 V, the linear displacement is almost twice larger than the nonlinear displacement. It can be explained by the fact that the stiffness of the V-beam system with two fixed ends increases rapidly with the displacement value  $Y_1$ . Due to the large axial internal force, the stiffness of V-beams in the moving direction of the shuttle (i.e. in  $Y$  direction) will increase.

In contrast, the results of calculation in the case of nonlinear displacement and simulation have negligible deviations (approximately 7.7% at 16 V). Especially at the voltages are lower than 12 V, the displacements almost match together (see Figure 10). In other words, the proposed formula (i.e. formula number 14) has a much higher accuracy than the traditional linear formula. It enables to attain a more accurate calculation of microdevices using the V-shaped actuators.

In our experiment, one EVA structure (dimensions are given in Table 1) was fabricated as mentioned in Section 3.1. The CCD camera images of this structure while operating at the voltage of 16 V are illustrated in Figure 7. The measured displacements at different voltages are shown in the graph of Figure 11. At each driving voltage, the experimental

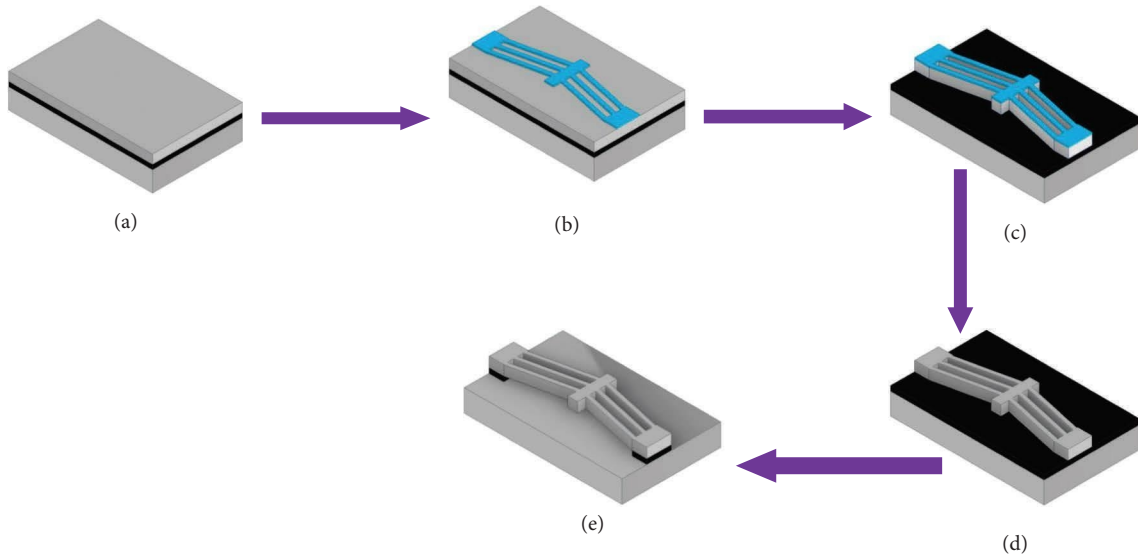


FIGURE 4: The fabrication process of the V-shaped actuator. (a) Cleaning the SOI wafer; (b) photolithography and developing; (c) deep reactive ion etching; (d) cutting and removing photoresist; (e) vapor HF etching.

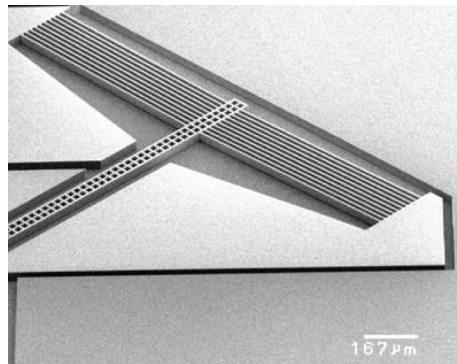


FIGURE 5: SEM image of fabricated EVA.

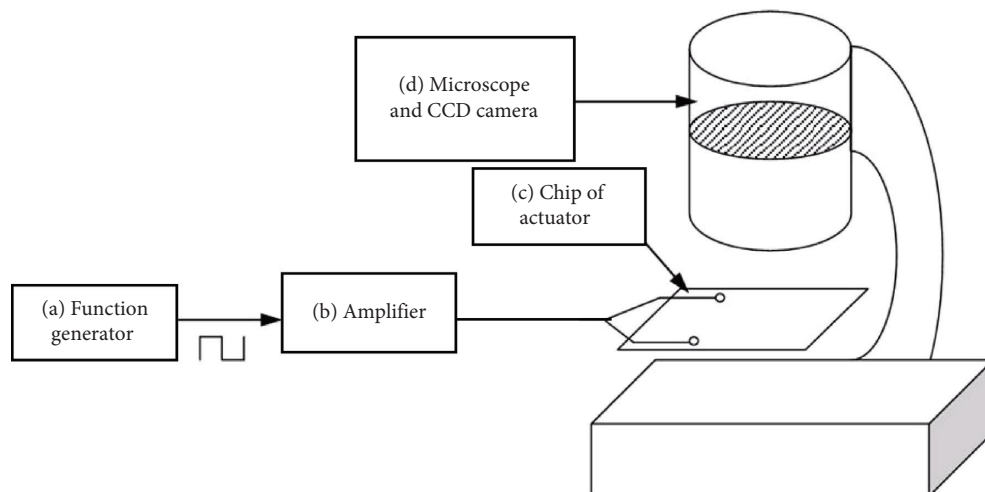


FIGURE 6: The diagram of displacement measuring system. (a) Function generator; (b) amplifier; (c) chip of V-shaped actuator; (d) microscope connected to CCD camera.

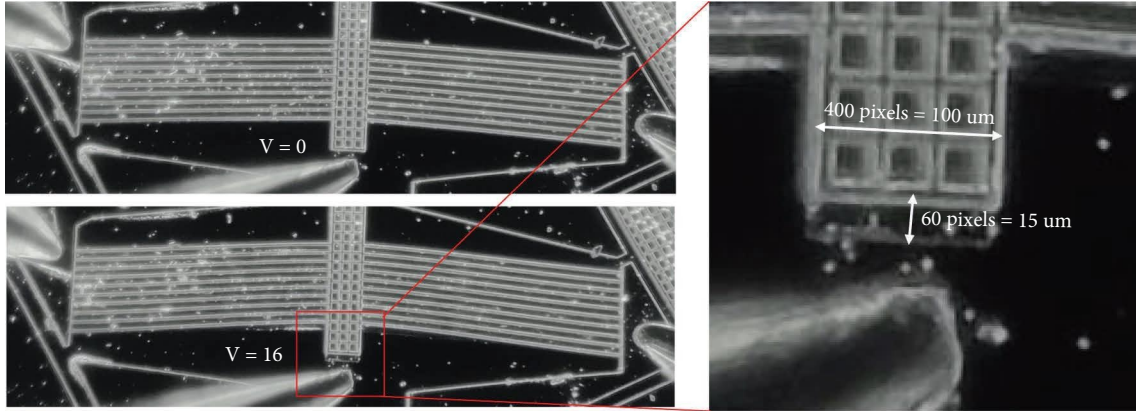


FIGURE 7: The EVA after fabricating and the measured displacement at the voltage of 16 V.

TABLE 1: Geometry dimensions of EVA.

$L$ ( $\mu\text{m}$ )	$h$ ( $\mu\text{m}$ )	$w$ ( $\mu\text{m}$ )	$g_a$ ( $\mu\text{m}$ )	$\theta$ ( $^\circ$ )	$n$
750	30	6	4	2	10

TABLE 2: Material parameters of silicon.

$d$ ( $\text{kg}/\text{m}^3$ )	$E$ (GPa)	$k_a$ (W/m·K)	$C_p$ (J/kg·K)	$\rho_0$ ( $\Omega\cdot\text{m}$ )	$\lambda$ (1/K)
2330	169	0.0257	712	$148 \times 10^{-6}$	$1.25 \times 10^{-3}$

TABLE 3: Material parameters depend on temperature [16].

$T$ (K)	$k$ (W/m·K)	$\alpha$ ( $10^{-6}$ 1/K)
300	156	2.62
400	105	3.25
500	80	3.61
600	64	3.84
700	52	4.02
800	43	4.15
900	36	4.18
1000	31	4.26
1100	28	4.32
1200	26	4.38
1300	25	4.44

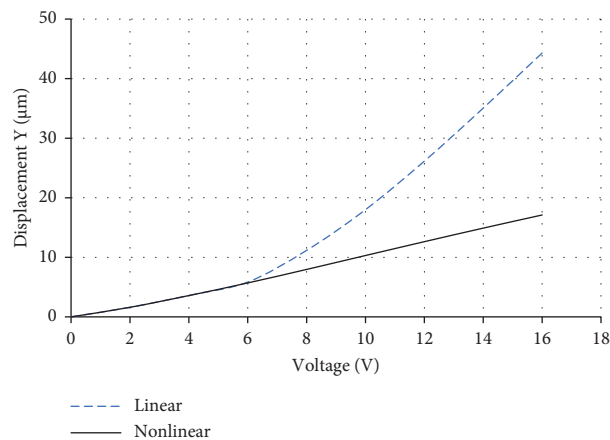


FIGURE 8: Comparison between linear and nonlinear displacements.

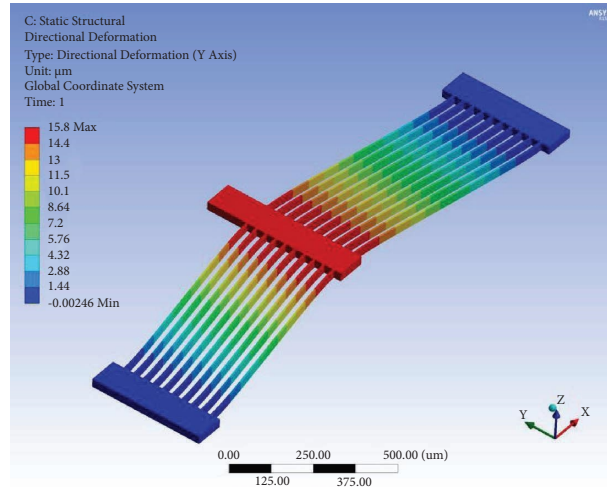


FIGURE 9: Simulating displacement at the voltage of 16 V.

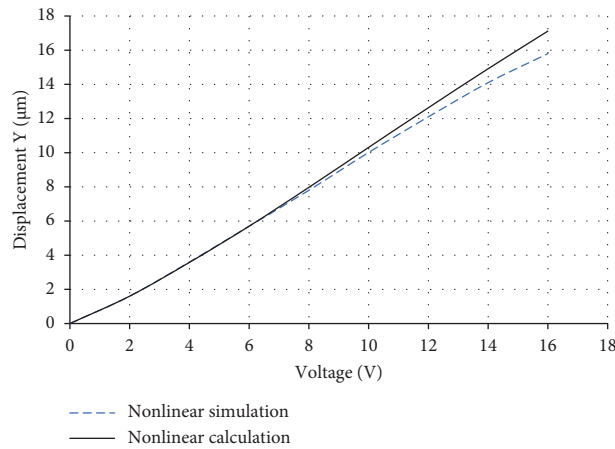


FIGURE 10: Comparison between nonlinear calculation and simulation.

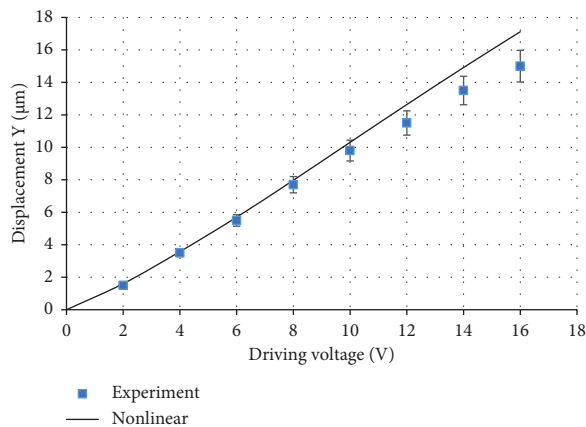


FIGURE 11: Comparison of nonlinear calculation and experimental displacements.

displacements are determined four times for 4 similar V-shaped actuators and then averaged. The whiskers in Figure 11 illustrate the upper and under measured values.

As illustrated in Figure 11, the theoretical and experimental displacements have minor deviations while applying voltage is lower than 10 V. At the voltage of 10 V, the relative



displacement deviation in both theoretical and measured is an inconsiderable, about 5%. When the voltage is larger than 10 V, the displacement deviation increases and reaches 12.4% at 16 V. This difference can be explained by two reasons: firstly, loss of voltage at the contact point when measuring directly by probes in this case; secondly in practice, the heat loss from the beams to the ambient is larger than the finite difference calculation method. Anyway, the theoretical displacement results calculated by formula (19) are quite accurate when compared with the experimental ones and clearly achieve higher accuracy than the traditional linear formula.

An example to show the advantage of formula (19) while applying in V-beam design: Need to determine the preliminary beam length  $L$  of the EVA aim to achieve a displacement of  $15\ \mu\text{m}$  corresponding to a driving voltage of 15 V (the other dimensions of the beam are assumed to be fixed as in Table 1). The linear and the nonlinear models will give the results  $L_1 = 235\ \mu\text{m}$  and  $L_2 = 690\ \mu\text{m}$ , respectively. Here, the nonlinear formula has given more accurate results as the beam length  $L_2$ . This helps us to significantly decrease the time of design and calculation as well as reduce the fabrication cost of the microdevices.

In general, the experimental results have demonstrated the advantage of the nonlinear displacement model with much higher accuracy than the linear model, as well as the tolerance of this model compared to experiment is significantly decreased. However, the error between the nonlinear formula and experiment is still large while applying higher driving voltage. The reasons can be explained as: (i) the theoretical heat transfer model used some assumptions to simplify as shown in [12]; (ii) when the driving voltage increases, the temperature on the beam also is larger, leading to nonlinear change of material properties such as thermal expansion coefficient and resistivity.

Obviously, the nonlinear model is better and more reliable than the linear formula of the previous publication [12]. Therefore, the proposed nonlinear displacement formula can help design result achieves better accuracy, allows to reduce design cycle process as well as trial fabrication time, ultimately reducing manufacturing cost.

## 5. Conclusion

Due to the geometrical deformation of the EVA when working at a high voltage condition, nonlinear displacement phenomenon will occur. The article has proposed and contributed the formula for calculating the nonlinear displacement of the EVA to improve the accuracy. Some featured results can be summarized as following:

- (i) By solving the differential equations, the formula for calculating the nonlinear displacement of the EVA has been figured out when considering the axial deformation of the V-beam.
- (ii) Comparing the linear/nonlinear/simulation displacements of the same EVA structure to confirm the advantages of the nonlinear displacement formula as mentioned.

- (iii) Experimental displacement of similar EVA structures was conducted. The measured results have proved that the significantly accuracy of the proposed nonlinear formula (the maximum relative deviation compared with experiment is approximate 12.4% at voltage of 16 V).

This nonlinear model can be used to design and optimize the microsystems driven by the EVA structure, aim to obtain high-precision requirements when working such as: in microtransportation system, material testing microsize device, the positioning system during the assembly and movement of microspecimen, etc.

To be as a suggestion, this work can be further developed by applying optimal algorithms to find out the desired V-beam dimensions according to the required displacement. In addition, it can be improved and applied to calculate nonlinear displacements for others like U-shaped or Z-shaped electrothermal microactuators.

## Data Availability

No data supporting the results.

## Conflicts of Interest

The authors declare that there are no conflicts of interest regarding the publication of this paper.

## Acknowledgments

This work was supported by the Centennial SIT Action for the 100th anniversary of the Shibaura Institute of Technology to enter the top ten Asian Institute of Technology. The research would like to express our gratitude for the support from the Ministry of Science and Technology, Vietnam; Hanoi University of Science and Technology, as well as the members of KomLab.

## References

- [1] A. Potekhina and C. Wang, "Review of electrothermal actuators and applications," *Actuators*, vol. 8, no. 4, p. 69, 2019.
- [2] Z. Zhang, Y. Yu, X. Liu, and X. Zhang, "A comparison model of V- and Z-shaped electrothermal microactuators," in *Proceedings of the 2015 IEEE International Conference on Mechatronics and Automation, ICMA 2015*, pp. 1025–1030, Beijing, China, September 2015.
- [3] P. Shivhare, G. Uma, and M. Umopathy, "Design enhancement of a chevron electrothermally actuated microgripper for improved gripping performance," *Microsystem Technologies*, vol. 22, no. 11, pp. 2623–2631, 2016.
- [4] T. Hu, Y. Zhao, X. Li, Y. Zhao, and Y. Bai, "Design and fabrication of an electro-thermal linear motor with large output force and displacement," in *Proceeding of the 2016 IEEE SENSORS*, pp. 1–3, Orlando, FL, USA, October 2016.
- [5] H. D. Espinosa, Y. Zhu, and N. Moldovan, "Design and operation of a MEMS-based material testing system for nanomechanical characterization," *Journal of Microelectromechanical Systems*, vol. 16, no. 5, pp. 1219–1231, 2007.

- [6] T. Hu, Y. Zhao, X. Li, Y. Zhao, and Y. Bai, "Integration design of MEMS electro-thermal safety-and-arming devices," *Microsystem Technologies*, vol. 23, no. 4, pp. 953–958, 2017.
- [7] Z. Zhang, W. Zhang, Q. Wu, Y. Yu, X. Liu, and X. Zhang, "Closed-form modelling and design analysis of V- and Z-shaped electrothermal microactuators," *Journal of Micromechanics and Microengineering*, vol. 27, no. 1, Article ID 015023, 2017.
- [8] Z. Zhang, Y. Yu, X. Liu, and X. Zhang, "Dynamic modelling and analysis of V- and Z-shaped electrothermal microactuators," *Microsystem Technologies*, vol. 23, no. 8, pp. 3775–3789, 2017.
- [9] C. D. Lott, T. W. McLain, J. N. Harb, and L. L. Howell, "Modeling the thermal behavior of a surface-micromachined linear-displacement thermomechanical microactuator," *Sensors and Actuators A: Physical*, vol. 101, no. 1–2, pp. 239–250, 2002.
- [10] T. Shan, X. Qi, L. Cui, and X. Zhou, "Thermal behavior modeling and characteristics analysis of electrothermal microactuators," *Microsystem Technologies*, vol. 23, no. 7, pp. 2629–2640, 2017.
- [11] D. T. Nguyen, K. T. Hoang, and P. H. Pham, "Heat transfer model and critical driving frequency of electrothermal V-shaped actuators," *Advances in Engineering Research and Application*, vol. 104, pp. 394–405, 2020.
- [12] K. T. Hoang, D. T. Nguyen, and P. H. Pham, "Impact of design parameters on working stability of the electrothermal V-shaped actuator," *Microsystem Technologies*, vol. 26, no. 5, pp. 1479–1487, 2020.
- [13] Y. Zhu, A. Corigliano, and H. D. Espinosa, "A thermal actuator for nanoscale in situ microscopy testing: design and characterization," *Journal of Micromechanics and Microengineering*, vol. 16, no. 2, pp. 242–253, 2006.
- [14] M. Pustan, R. Chiorean, C. Birleanu et al., "Reliability design of thermally actuated MEMS switches based on V-shape beams," *Microsystem Technologies*, vol. 23, no. 9, pp. 3863–3871, 2017.
- [15] E. T. Enikov, S. S. Kedar, and K. V. Lazarov, "Analytical model for analysis and design of V-shaped thermal microactuators," *Journal of Microelectromechanical Systems*, vol. 14, no. 4, pp. 788–798, 2005.
- [16] R. Hull, *Properties of Crystalline Silicon*, INSPEC, London, UK, 1999.